NMDA Receptor-mediated CaMKII/ERK Activation Contributes to Renal Fibrosis

Jingyi Zhou
Zhejiang University School of Medicine First Affiliated Hospital https://orcid.org/0000-0001-5833-081X
Shuaihui Liu
Zhejiang University School of Medicine First Affiliated Hospital
Luying Guo
Zhejiang University School of Medicine First Affiliated Hospital
Rending Wang
Zhejiang University School of Medicine First Affiliated Hospital
Jianghua Chen
Zhejiang University School of Medicine First Affiliated Hospital
Jia Shen (jiashen@zju.edu.cn)
Zhejiang University

Research article

Keywords: Renal fibrosis, NMDA receptor, CaMKII, ERK

Posted Date: July 16th, 2020

DOI: https://doi.org/10.21203/rs.2.16509/v3

Version of Record: A version of this preprint was published on September 9th, 2020. See the published version at https://doi.org/10.1186/s12882-020-02050-x.

Abstract

Background: Renal fibrosis (RF) results in renal function impairment and eventually kidney failure. We found that N-methyl-D-aspartate receptor (NMDAR) played an important role during RF. However, its mechanism of action is yet to be deciphered.

Methods: Acute RF was induced in mice by unilateral ureteral obstruction (UUO). NR1, which is the functional subunit of NMDAR, was downregulated using lentiviral vector-mediated shRNA interference. Histological changes were observed by Masson's trichrome staining. Expression of NR1, fibrotic and EMT markers were measured by immunohistochemistry and western blot analysis. HK-2 cells were incubated with TGF-β, and NMDAR antagonist MK-801 and Ca2+/calmodulin-dependent protein kinase II (CaMKII) antagonist KN-93 administration were further included in this study for pathway determination. Expression of NR1, total and phosphorylated CaMKII, total and phosphorylated ERK were measured using western blot and immunofluorescent assays. Chronic renal fibrosis was introduced by sublethal ischemia-reperfusion injury in mice, and oral NMDAR inhibitor dextromethorphan (DXM) administration was performed.

Results: NR1 expressions were upregulated in both obstructed kidneys and TGF-β treated HK-2 cells. NR1 knockdown, MK801 and KN93 reduced the fibrotic morphology in vivo and in vitro respectively, and companied with the downregulated ERK activation, while KN93 administration had no effect on NR1 and CaMKII levels. Mice in the DXM group had better preservation of kidney structures and corticomedullary volumes.

Conclusions: NMDAR participates in both acute and chronic renal fibrogenesis via CaMKII/ERK activation, and is a potential therapeutic target for renal fibrosis.

Background

Acute kidney injury (AKI) affects approximately 20% of hospitalized patients [1]. A proportion of AKI patients will undergo maladaptive repair of their kidneys. This contributes to the ongoing fibrotic processes which progresses over time to chronic nephropathy. Chronic kidney diseases (CKD) has a prevalence of 10.8% in China [2] and 14.0% in the USA [3]. Renal fibrosis (RF) is a common final outcome of progressive AKI nephropathy and for nearly all types of CKD [4,5]. Clinical studies have demonstrated that renal function correlates more closely with fibrosis compared to glomerular damage [6], and is a major exacerbating factor for renal dysfunction [7]. After kidney damage, the fibrotic process is initiated with impaired kidney repair, sustained inflammation, activation of myofibroblasts and accumulation of extracellular matrix (ECM) [5,8]. Alpha-SMA (α-SMA) is often used as a marker of myofibroblast formation [9]. type I collagen (COL1A1) and fibronectin indicate enhanced deposition of ECM during fibrogenesis [10,11]. S100 calcium-binding protein A4 (S100A4), also called fibroblast-specific protein 1, is considered a specific marker of fibroblasts in tissue remodeling [12]. The transition of tubular epithelial cells into cells with mesenchymal features, also known as epithelial-to-mesenchymal transition (EMT), is observed

during fibrosis [13]. Increased expression of transcription factors that are associated with EMT correlates with disease progression [14, 15]. Snail is a prominent inducer of EMT and E-cadherin loss is one of the hallmarks of EMT [16]. The pathological changes that occur during renal fibrosis eventually leads to renal failure [17]. Hence, therapeutically targeting RF may be a promising strategy to treat kidney diseases. At present, no effective treatment strategies are currently available.

N-methyl-D-aspartate receptor (NMDAR) is an ionotropic glutamate receptor. It has been well-studied in the central nervous system (CNS), and has a vital role in development, learning and memory. In addition, it can induce Ca^{2+} overload during multiple pathological conditions [18,19]. Functional NMDAR is a tetrameric complex consisting of two NR1 subunits and two NR2 and/or NR3 subunits. The subunits are encoded by seven genes: one for NR1, four for NR2 (A-D), and two For NR3 (A-B) [20]. All subunits have a conserved domain organization including an extracellular amino-terminal domain, an extracellular ligand binding domain, a transmembrane domain and an intracellular carboxy-terminal domain [20,21]. The obligatory NR1 subunit binds glycine and d-serine and had been demonstrated by several studies widely expressed in the kidneys, bone, heart and other tissues, in addition to the CNS. Hence, the functional role of NMDAR outside of the CNS has garnered research interest [21]. Growing evidence suggests that NMDAR plays an important role in numerous processes such as proliferation, apoptosis, cell adhesion and migration, actin rearrangement, cell growth and differentiation, and regulation of hormone secretion. In the kidney, NMDAR expression has been detected in the glomeruli and tubules [22,23]. NMDAR expression is induced by various kidney pathological processes, including acute ischemia-reperfusion injury (IRI) [24,25] and diabetic nephropathy [26-28]. Whether NMDAR expression is associated with RF is yet to be deciphered [29].

We found that NR1 expression was higher in kidney fibrotic biopsy samples compared to kidneys from healthy donors (unpublished data). Hence, we designed this study to understand the mechanistic role of NMDAR in acute fibrogenesis using *in vivo* models of ureter obstruction and *in vitro* TGF-β administration. Furthermore, to understand the role of NMDAR *in vivo*, we administered mice with dextromethorphan (DXM), which is widely used in the clinic as an NMDAR inhibitor. We then observed the effect of DXM on chronic fibrosis after IRI.

Methods

Animals

Eight-week-old C57BL/6 mice (20-25 grams, half male) were purchased from the Experimental Animal Center in Zhejiang Medical Academy of Sciences and housed in a temperature-controlled room with 12-hour day/night cycles. The mice had free access to standard food and water throughout the study. All animal studies were done in compliance with the regulations and guidelines of Zhejiang University institutional animal care and conducted according to the AAALAC and the IACUC guidelines (Permit Number: 2016-205, date of approval: 26 Feb 2016). Animals were euthanized with overdose anesthesia (500 mg/kg sodium pentobarbital) and CO_2 incubation after experimentation.

Retrograde Ureteral Lentivirus Delivery and Unilateral Ureteral Obstruction (UUO)

Mice were anesthetized using 50 mg/kg sodium pentobarbital by intraperitoneal injection. Mice were then infused with lentivirus 7 days prior to UUO as previously described. Briefly, mice were anesthetized, and a midline abdominal incision was performed on the left kidney and the terminal ureters were obstructed. Then, 5×10^7 IU/100 μl filter-purified scrambled-shRNA (Scr-sh group, n=6) or NR1-shRNA (NR1-sh Group, n=6) lentivirus cocktail (forward: 5'-CACCGGTACCCATGTCATCCCAAATCGAAATTTGGGATGACATGGGTACC-3' and reverse: 5'-AAAAGGTACCCATGTCATCCCAAATTTCGATTTGGGATGACATGGGTACC-3') purchased from NovoBio Biotechnology Co., Shanghai, China [22] was infused through the ureters for 5 min via an intrathecal catheter attached to a micro-syringe (Hamilton, Franklin, Massachusetts) pump (WPI). After 7 days, mice were re-anesthetized and a midline abdominal incision was performed on the left kidney. The left ureters were double ligated with 4-0 silk surgical sutures [30].

Human proximal tubule (HK-2) cell culture and drug treatment

HK-2 cells (American Type Culture Collection, Manassas, Virginia) were grown in keratinocyte medium (Thermofisher, Waltham, Massachusetts) with 10% FBS in a 5% CO_2 humidified incubator at 37°C. Cells were then treated with recombinant human TGF-β (100 ng/ml, R&D System, Minneapolis, Minnesota) for 48 h with a combination of NMDA (50 μM, Tocris, Minneapolis, Minnesota), MK-801 (10 μM, Tocris), or KN-93 (10 μM, Tocris).

Ischemia/reperfusion (IR) mouse model and DXM Administration

Mice were anesthetized and then a midline abdominal incision was performed on the right kidney. The right renal artery was isolated from the renal vein carefully and then clapped for 60 min. Mice were then divided randomly into the IR group (n=6), low-dose DXM group (Yiling, Hebei Province, LD group, 1 mg/ml in drinking water, n=6), moderate-dose DXM group (MD group, 2 mg/ml in drinking water, n=6), and high-dose DXM group (HD group, 3 mg/ml in drinking water, n=6). Mice were then euthanized 28 days post-IR.

Masson's Trichrome Staining, Immunohistochemistry and Immunofluorescent assays

Seven days post-UUO, mice were anesthetized, and the obstructed kidneys were harvested. Paraffin sections were stained with Masson's trichrome or labeled with antibodies against TGF-β1 (Cell Signaling Technology, Danvers, Massachusetts), alpha-smooth muscle actin (Abcam, Cambridge, Massachusetts), COL1A1 (Abcam), S100A4 (Abcam) or Fibronectin (Abcam). Frozen sections and fixed cells were labeled with antibodies against NR1 (ThermoFisher), p- or total CaMKII (Abcam), p- or total extracellular signal-regulated kinase (ERK, Abcam), Snail (Abcam) or E-cadherin (Abcam) and then incubated with the relevant secondary antibodies for immunohistochemistry or immunofluorescence (Abcam). Nuclei were stained with 4,6-diamidino-2-phenylindole (DAPI, ThermoFisher) for immunofluorescent assays.

Western blotting Analysis

Kidneys and cells were homogenized in RIPA lysis buffer with protease and phosphatase inhibitor cocktail (Cell Signaling Technology). Total protein was then separated by SDS-PAGE and blotted with antibodies against α-SMA, COL1A1, S100A4, Fibronectin, NR1, p- or total CaMKII, p- or total ERK. The membranes were scanned and analyzed using the Gel Doc XR imaging system (Bio-Rad Laboratories, Hercules, California).

Statistical analysis

Data values were presented as mean ± SD. Area of fibrosis and positive staining in tissue sections was measured with Image J software and was shown as percentages. Standard ANOVA with Bonferroni test was performed using GraphPad Prism 6.0. Two-tailed Student's *t* test was used for other data types. Differences were considered statistically significant at $P<0.05$.

Results

NR1 expression was upregulated by ureteral obstruction

NR1 expression was significantly upregulated in obstructed kidneys as determined by western blotting (Figure 1A). The higher interstitial volumes and corticomedullary atrophies were also found in the obstructed kidneys determined by Masson's trichrome staining (Figure 1B).

NR1 knockdown partially suppressed the fibrotic process and markers in obstructed kidneys

Retrograde ureteral delivery of NR1-shRNA (NR1-sh) reduced NR1 expression levels in kidneys with or without obstruction injury (*$P < 0.01$ *versus* Control group). NR1 knockdown reduced interstitial volumes and the corticomedullary atrophy compared with UUO and Scr-sh groups (Figure 1B).

The overexpression of these fibrotic markers induced by UUO were not totally reversed by NR1 knockdown. Kidneys infused with NR1-shRNA had a significant reduction in α-SMA, S100A4, fibronectin and COL1A1 expression levels compared with the kidneys in UUO and Scr-sh groups, while S100A4 and COL1A1 expression levels were slightly higher in the Scr-sh group but had no statistical significance (*$P > 0.05$ *versus* Control group, Figure 2).

NR1 knockdown partially inhibited EMT marker expression changes after UUO injury

Snail and E-cadherin had opposite expression trends after UUO injury (Figure 3). Snail expression levels increased sharply in obstructed kidneys, while E-cadherin expression levels were reduced. Snail overexpression and E-cadherin down-regulation were both partly inhibited by NR1 knockdown. Snail expression levels in the NR1-sh group were still higher compared to normal kidneys, while E-cadherin expression levels were lower.

NMDAR activation induced phosphorylation of CaMKII and ERK in TGF-β treated HK-2 cells

TGF-β treated HK-2 cells were used as an *in vitro* fibrosis model. In untreated cells, NR1 was expressed at low levels in the cytoplasm and less on the membrane (Figure 4A). TGF-β treatment increased NR1 signals which localized both in the cytoplasm and on the membrane, and were correlated with higher CaMKII and ERK phosphorylation (Figure 4). Both NMDAR antagonist MK801 and CaMKII antagonist KN93 reduced CaMKII and ERK phosphorylation levels respectively in the presence of TGF-β, without NR1 signal changes.

NR1 knockdown inhibited CaMKII/ERK activation in UUO-induced renal fibrosis

Total and phosphorylated CaMKII and ERK levels after UUO operation were measured using immunoblotting (Figure 5). Total CaMKII and ERK expression levels in the obstructed kidneys were higher compared to control kidneys, and were not affected after NR1 knockdown. In addition, CaMKII and ERK phosphorylation levels increased after UUO injury, while NR1 knockdown significantly reduced their phosphorylation levels. A more notable reduction in phosphorylation was observed for CaMKII.

Oral NMDAR inhibitor dextromethorphan protected kidneys from chronic fibrosis after IR injury

IRI was performed on the right kidneys of mice and chronic RF was induced soon afterwards. Varying degrees of recovery were observed after DXM administered at different dosages. Kidneys from mice treated with DXM were larger in size compared to controls. Mice that were administered the highest dose of DXM had nearly the same sized kidneys as normal mice and were consistent with Masson's staining results (Figure 6). Mice in the DXM group had better preservation of kidney structures and corticomedullary volumes. The differences in serum creatinine levels between the groups were not significant ($P > 0.05$).

Discussion

In the present study, we demonstrated that 1) NMDAR was overexpressed during renal fibrosis induced by ureteral obstruction *in vivo* and by TGF-β treatment *in vitro*, 2) NMDAR activation induced the phosphorylation of CaMKII and ERK, 3) both NR1 inhibition and knockdown significantly reduce the phosphorylation levels of CaMKII and ERK, 4) CaMKII inhibition reduces the phosphorylation of ERK but has no effect on NR1 expression, 5) oral administration of NMDAR inhibitor suppresses the chronic renal fibrosis after sublethal ischemic injury.

Fibrosis is associated with a reduction in the functional structures of the kidney, which eventually leads to organ failure. Renal fibrosis is the common outcome of all progressive nephropathies. The initial therapeutic strategy for the treatment of renal fibrogenesis was to target the renin angiotensin system (using angiotensin converting enzyme inhibitors (ACEI) or angiotensin receptor blockers (ARB)) [31]. However, this approach was not efficacious in treating renal fibrosis. Later, several studies demonstrated that TGF-β played a central role in fibrosis [32]. However targeting TGF-β is problematic due to its diverse roles in cell proliferation and differentiation, wound healing and in the immune system [33]. Although several targeting strategies have been proven effective in renal fibrosis animal models, there are no novel

therapeutic targets that have demonstrated safety and efficacy in preventing or alleviating renal fibrosis in humans [34]. One important reason is that rodent models often do not fully mimic the human clinical situation and only a few studies have used more than one model to verify their findings [35]. There are multiple mice models of renal fibrosis based on different inducements. Surgical animal models have been used to reduce kidney mass, UUO and IRI. Kidney mass reduction could be achieved by 5/6 nephrectomy, however it is less likely to mimic the human clinical situation [36]. UUO and IRI are hence the closest models to replicate human disease, thus we used both models to determine the efficacy of NMDAR in renal fibrosis. The UUO model is the most widely used because of its rapid development of tubular atrophy, interstitial fibrosis and matrix deposition. However, this absolute obstruction is very rarely observed in humans. Nonetheless, the UUO model reproduces a typical fibrotic sequence of events including hemodynamic changes, interstitial inflammatory infiltration, and tubular cell death [37]. Our results demonstrated that TGF-β (Supplemental Figure 1) and NR1 were increased after UUO injury, and NR1 knockdown protected kidneys from acute injury after UUO with a stable expression of TGF-β (Supplemental Figure 1). A sixty-minute ischemia induces severe hypoxia and cell damage [38], and is exacerbated by reperfusion, which eventually leads to fibrosis [39]. Hence, we used the IRI model to mimic chronic progression from injury to fibrosis. Ischemic kidneys from mice treated with DXM had reduced histological features 28 days after reperfusion. The effect of DXM on renal fibrosis was dose-dependent, with kidneys from mice treated with a high-dose of DXM exhibiting no significant differences from kidneys from control mice.

EMT of tubular epithelial cells (TECs) is a feature observed during renal fibrosis [13]. TECs injury results in loss of functional parenchyma and induces pathological processes including EMT [13]. Injury-induced EMT eventually leads to fibrosis [40]. Preventing the initiation of EMT results in the reduction of myofibroblast recruitment and extracellular matrix deposition, and hence preserves functional TECs and improves organ function [13]. In this study, we demonstrated that EMT markers were altered after UUO-induced injury along with NMDAR activation. NR1 knockdown reduced the changes in expression levels of Snail and E-cadherin. This suggested that NMDAR was a target for EMT inhibition.

In addition, we investigated the downstream pathway of NMDAR using HK-2 cells by TGF-β treatment. Immunofluorescent assays demonstrated low expression levels of NR1 in the cytoplasm and even lower levels on the membranes of untreated HK-2 cells. Cytoplasmic localization of NR1 is associated with its production in the endoplasmic reticulum and maturation, while membrane anchoring is associated with maturation and function of NMDARs [41]. TGF-β increases NR1 expression and localization in both the cytoplasm and membrane. CaMKII is one of the key protein kinases that mediates changes in intracellular Ca^{2+} levels [42]. CaMKII phosphorylation increases significantly during fibrogenesis and plays a key role in TGF-β-induced fibrogenic cascades [43]. In addition to fibrosis, CaMKII mediates oxidative stress, which is pivotal for IRI progression [44]. CaMKII has been demonstrated to be activated by NMDAR in the CNS as an intracellular sensitive kinase [45], however its function in the kidneys has not been deciphered. Our study demonstrated that CaMKII was phosphorylated by activated NMDAR and NR1

inhibition reduced CaMKII phosphorylation. In the UUO model, NR1 knockdown reduced CaMKII phosphorylation but had no effect on total CaMKII expression.

ERK is a widely expressed intracellular signaling protein kinase and is involved in diverse biological functions [46]. Phosphorylation at Thr^{202}/Tyr^{204} residues results in its activation. ERK has been demonstrated to be involved in renal fibrosis, but its role has been controversial. Majority of studies have shown that ERK acts as a pro-fibrotic factor important for inflammatory responses [47], TGF-β/Smad signaling [48], ECM and myofibroblast accumulation [49,50]. In addition, ERK has recently been shown to participate in EMT progression, and inhibition of ERK ameliorates renal interstitial fibrosis by suppressing tubular EMT [51,52]. However, Jang et.al. demonstrated that activation of ERK accelerates renal tubular epithelial cell repair and inhibits fibrogenesis following IRI [53]. This is consistent with previous studies that showed the phosphorylation of ERK was protective and promoted the growth of renal tubular epithelium but induced apoptosis in renal fibroblasts [54]. We found that ERK was activated upon CaMKII phosphorylation after NRI overexpression using both *in vitro* and *in vivo* fibrosis models. NR1 shRNA knockdown or inhibition with MK801 reduced the phosphorylation levels of ERK. Inhibition of CaMKII reduced ERK phosphorylation, regardless of NR1 expression in the cytoplasm and on the membrane.

Conclusions

In summary, NMDAR participates in renal fibrogenesis by activating the CaMKII/ERK pathway. NMDAR inhibition via oral administration shows promise in protecting against fibrosis after IRI. We believe that NMDAR is a potential therapeutic target, however more studies are required to substantiate our findings.

List Of Abbreviations

AKI: acute kidney injury

CKD: chronic kidney diseases

RF: renal fibrosis

NMDARs: N-methyl-D-aspartate receptors

UUO: unilateral ureteral obstruct

α-SMA: α-smooth muscle actin

ECM: extracellular matrix

EMT: epithelial-to-mesenchymal transition

CaMKII: Ca^{2+}/calmodulin-dependent protein kinase II

IR: ischemia/reperfusion

DXM: dextromethorphan

Declarations

Ethics approval and consent to participate

All experimental procedures were performed according to protocols approved by the Animal Care and Use Committee at Zhejiang University.

Consent for publication

Not applicable

Availability of data and materials

The datasets used and/or analyzed during the current study are available from the corresponding author on reasonable request.

Competing interests

Not applicable

Funding

This research was supported by National Natural Science Foundation of China (81770719, 81870510 and 81770750) and Natural Science Foundation of Zhejiang Province (LQ18H050002). These grants mainly helped us with purchase of animals and reagents, and animal housing.

Authors' contributions

JS and JC proposed, initiated and led the study. In addition, JS conceived and performed the *in vitro* experiments, and wrote the manuscript. JZ and LG performed the *in vivo* studies and analyzed the data. SL and RW assisted with the biopsies and *in vivo* studies, performed the surgical design, and provided helpful discussions. All authors provided final approval for submission of this manuscript.

Acknowledgements

We thank Prof. Xia Qiang and Prof. IC Bruce for constructive comments on our manuscript.

References

1. Levey AS, James MT. Acute Kidney Injury. *Ann Intern Med* 2017; **167**(9): ITC66-ITC80.
2. Zhang L, Wang F, Wang L, et al. Prevalence of chronic kidney disease in China: a cross-sectional survey. *Lancet* 2012; **379**(9818): 815-822.

3. Kidney Disease Statistics for the United States. https://www.niddk.nih.gov/health-information/health-statistics/kidney-disease, 2018.
4. Shu S, Wang Y, Zheng M, et al. Hypoxia and Hypoxia-Inducible Factors in Kidney Injury and Repair. *Cells* 2019; **8**(3).
5. Humphreys BD. Mechanisms of Renal Fibrosis. *Annu Rev Physiol* 2018; **80**: 309-326.
6. Gewin LS. Renal fibrosis: Primacy of the proximal tubule. *Matrix Biol* 2018; **68-69**: 248-262.
7. Duffield JS. Cellular and molecular mechanisms in kidney fibrosis. *J Clin Invest* 2014; **124**(6): 2299-2306.
8. Jager KJ, Fraser SDS. The ascending rank of chronic kidney disease in the global burden of disease study. *Nephrol Dial Transplant* 2017; **32**(suppl_2): ii121-ii128.
9. Nagamoto T, Eguchi G, Beebe DC. Alpha-smooth muscle actin expression in cultured lens epithelial cells. *Invest Ophthalmol Vis Sci* 2000; **41**:1122-1129.
10. Wright RD, Dimou P, Northey SJ, Beresford MW. Mesangial cells are key contributors to the fibrotic damage seen in the lupus nephritis glomerulus. *J Inflamm (Lond)*; 2019, 16:22.
11. Osterreicher CH, Penz-Osterreicher M, Grivennikov SI, et al. Fibroblast-specific protein 1 identifies an inflammatory subpopulation of macrophages in the liver. *Proc Natl Acad Sci USA*; 2011, **108**:308-313.
12. Van Vliet A, Baelde HJ, Vleming LJ, de Heer E, Bruijn JA. Distribution of fibronectin isoforms in human renal disease. *J Pathol*; 2001, **193**:256-262.
13. Lovisa S, LeBleu VS, Tampe B, et al. Epithelial-to-mesenchymal transition induces cell cycle arrest and parenchymal damage in renal fibrosis. *Nat Med* 2015; **21**(9): 998-1009.
14. Liu J, Zhong Y, Liu G, et al. Role of Stat3 Signaling in Control of EMT of Tubular Epithelial Cells During Renal Fibrosis. *Cell Physiol Biochem* 2017; **42**(6): 2552-2558.
15. Grande MT, Sanchez-Laorden B, Lopez-Blau C, et al. Snail1-induced partial epithelial-to-mesenchymal transition drives renal fibrosis in mice and can be targeted to reverse established disease. *Nat Med* 2015; **21**(9): 989-997.
16. Wang Y, Shi J, Chai K, Ying X, Zhou BP. The Role of Snail in EMT and Tumorigenesis. *Curr Cancer Drug Targets*; 2013, **13**:963-972.
17. Rockey DC, Bell PD, Hill JA. Fibrosis--a common pathway to organ injury and failure. *N Engl J Med* 2015; **372**(12): 1138-1149.
18. Paoletti P, Neyton J. NMDA receptor subunits: function and pharmacology. *Curr Opin Pharmacol* 2007; **7**(1): 39-47.
19. Xu H, Jiang H, Xie J. New Insights into the Crosstalk between NMDARs and Iron: Implications for Understanding Pathology of Neurological Diseases. *Front Mol Neurosci* 2017; **10**: 71.
20. Hardingham GE, Bading H. Synaptic versus extrasynaptic NMDA receptor signalling: implications for neurodegenerative disorders. *Nat Rev Neurosci* 2010; **11**(10): 682-696.
21. Marquard J, Otter S, Welters A, et al. Characterization of pancreatic NMDA receptors as possible drug targets for diabetes treatment. *Nat Med* 2015; **21**(4): 363-372.

22. Rastaldi MP, Armelloni S, Berra S, et al. Glomerular podocytes contain neuron-like functional synaptic vesicles. *FASEB J* 2006; **20**(7): 976-978.
23. Yang CC, Chien CT, Wu MH, et al. NMDA receptor blocker ameliorates ischemia-reperfusion-induced renal dysfunction in rat kidneys. *Am J Physiol Renal Physiol* 2008; **294**(6): F1433-1440.
24. Kim EY, Anderson M, Dryer SE. Sustained activation of N-methyl-D-aspartate receptors in podoctyes leads to oxidative stress, mobilization of transient receptor potential canonical 6 channels, nuclear factor of activated T cells activation, and apoptotic cell death. *Mol Pharmacol* 2012; **82**(4): 728-737.
25. Arora S, Kaur T, Kaur A, et al. Glycine aggravates ischemia reperfusion-induced acute kidney injury through N-Methyl-D-Aspartate receptor activation in rats. *Mol Cell Biochem* 2014; **393**(1-2): 123-131.
26. Shen J, Wang R, He Z, et al. NMDA receptors participate in the progression of diabetic kidney disease by decreasing Cdc42-GTP activation in podocytes. *J Pathol* 2016; **240**(2): 149-160.
27. Roshanravan H, Kim EY, Dryer SE. NMDA Receptors as Potential Therapeutic Targets in Diabetic Nephropathy: Increased Renal NMDA Receptor Subunit Expression in Akita Mice and Reduced Nephropathy Following Sustained Treatment with Memantine or MK-801. *Diabetes* 2016; **65**(10): 3139-3150.
28. Kundu S, Pushpakumar S, Sen U. MMP-9- and NMDA receptor-mediated mechanism of diabetic renovascular remodeling and kidney dysfunction: hydrogen sulfide is a key modulator. *Nitric Oxide* 2015; **46**: 172-185.
29. Bozic M, de Rooij J, Parisi E, Ortega MR, Fernandez E, Valdivielso JM. Glutamatergic signaling maintains the epithelial phenotype of proximal tubular cells. *J Am Soc Nephrol* 2011; **22**(6): 1099-1111.
30. Cachat F, Lange-Sperandio B, Chang AY, et al. Ureteral obstruction in neonatal mice elicits segment-specific tubular cell responses leading to nephron loss. *Kidney Int* 2003; **63**(2): 564-575.
31. Francois H, Chatziantoniou C. Renal fibrosis: Recent translational aspects. *Matrix Biol* 2018; **68-69**: 318-332.
32. Liu Y. Renal fibrosis: new insights into the pathogenesis and therapeutics. *Kidney Int* 2006; **69**(2): 213-217.
33. Morikawa M, Derynck R, Miyazono K. TGF-beta and the TGF-beta Family: Context-Dependent Roles in Cell and Tissue Physiology. *Cold Spring Harb Perspect Biol* 2016; **8**(5).
34. Montesi SB, Desogere P, Fuchs BC, et al. Molecular imaging of fibrosis: recent advances and future directions. *J Clin Invest* 2019; **129**(1): 24-33.
35. Boor P, Sebekova K, Ostendorf T, Floege J. Treatment targets in renal fibrosis. *Nephrol Dial Transplant* 2007; **22**(12): 3391-3407.
36. Nogueira A, Pires MJ, Oliveira PA. Pathophysiological Mechanisms of Renal Fibrosis: A Review of Animal Models and Therapeutic Strategies. *In Vivo* 2017; **31**(1): 1-22.
37. Chevalier RL, Forbes MS, Thornhill BA. Ureteral obstruction as a model of renal interstitial fibrosis and obstructive nephropathy. *Kidney Int* 2009; **75**(11): 1145-1152.

38. Adachi T, Sugiyama N, Gondai T, Yagita H, Yokoyama T. Blockade of Death Ligand TRAIL Inhibits Renal Ischemia Reperfusion Injury. *Acta Histochem Cytochem* 2013; **46**(6): 161-170.
39. Tanaka T. A mechanistic link between renal ischemia and fibrosis. *Med Mol Morphol* 2017; **50**(1): 1-8.
40. Qi R, Yang C. Renal tubular epithelial cells: the neglected mediator of tubulointerstitial fibrosis after injury. *Cell Death Dis* 2018; **9**(11): 1126.
41. Xia H, Hornby ZD, Malenka RC. An ER retention signal explains differences in surface expression of NMDA and AMPA receptor subunits. *Neuropharmacology* 2001; **41**(6): 714-723.
42. Zhang W, Chen DQ, Qi F, et al. Inhibition of calcium-calmodulin-dependent kinase II suppresses cardiac fibroblast proliferation and extracellular matrix secretion. *J Cardiovasc Pharmacol* 2010; **55**(1): 96-105.
43. An P, Tian Y, Chen M, et al. Ca(2+) /calmodulin- dependent protein kinase II mediates transforming growth factor-beta-induced hepatic stellate cells proliferation but not in collagen alpha1(I) production. *Hepatol Res* 2012; **42**(8): 806-818.
44. Zhang T, Zhang Y, Cui M, et al. CaMKII is a RIP3 substrate mediating ischemia- and oxidative stress-induced myocardial necroptosis. *Nat Med* 2016; **22**(2): 175-182.
45. Cervantes-Villagrana RD, Adame-Garcia SR, Garcia-Jimenez I, et al. Gbetagamma signaling to the chemotactic effector P-REX1 and mammalian cell migration is directly regulated by Galphaq and Galpha13 proteins. *J Biol Chem* 2019; **294**(2): 531-546.
46. Roux PP, Blenis J. ERK and p38 MAPK-activated protein kinases: a family of protein kinases with diverse biological functions. *Microbiol Mol Biol Rev* 2004; **68**(2): 320-344.
47. Basu RK, Hubchak S, Hayashida T, et al. Interdependence of HIF-1alpha and TGF-beta/Smad3 signaling in normoxic and hypoxic renal epithelial cell collagen expression. *Am J Physiol Renal Physiol* 2011; **300**(4): F898-905.
48. Zhu Y, Gu J, Zhu T, et al. Crosstalk between Smad2/3 and specific isoforms of ERK in TGF-beta1-induced TIMP-3 expression in rat chondrocytes. *J Cell Mol Med* 2017; **21**(9): 1781-1790.
49. Qin J, Mei WJ, Xie YY, et al. Fluorofenidone attenuates oxidative stress and renal fibrosis in obstructive nephropathy via blocking NOX2 (gp91phox) expression and inhibiting ERK/MAPK signaling pathway. *Kidney Blood Press Res* 2015; **40**(1): 89-99.
50. Cheng X, Zheng X, Song Y, et al. Apocynin attenuates renal fibrosis via inhibition of NOXs-ROS-ERK-myofibroblast accumulation in UUO rats. *Free Radic Res* 2016; **50**(8): 840-852.
51. Strippoli R, Loureiro J, Moreno V, et al. Caveolin-1 deficiency induces a MEK-ERK1/2-Snail-1-dependent epithelial-mesenchymal transition and fibrosis during peritoneal dialysis. *EMBO Mol Med* 2015; **7**(1): 102-123.
52. Wu Y, Wang L, Deng D, et al. Renalase Protects against Renal Fibrosis by Inhibiting the Activation of the ERK Signaling Pathways. *Int J Mol Sci* 2017; **18**(5).

53. Jang HS, Han SJ, Kim JI, et al. Activation of ERK accelerates repair of renal tubular epithelial cells, whereas it inhibits progression of fibrosis following ischemia/reperfusion injury. *Biochim Biophys Acta* 2013; **1832**(12): 1998-2008.
54. Pat B, Yang T, Kong C, et al. Activation of ERK in renal fibrosis after unilateral ureteral obstruction: modulation by antioxidants. *Kidney Int* 2005; **67**(3): 931-943.

Supplemental Figure Legend

Supplemental Figure 1 Immunohistochemical staining of TGF-β1 in kidneys from Control (Con) group, UUO group, UUO + NR1-sh group and UUO + Scr-sh group (A) and quantitative analysis (B). Representative image out of n = 6 individual samples per group. Origin magnification: ×200. Scale bar = 100 μm.

Figures

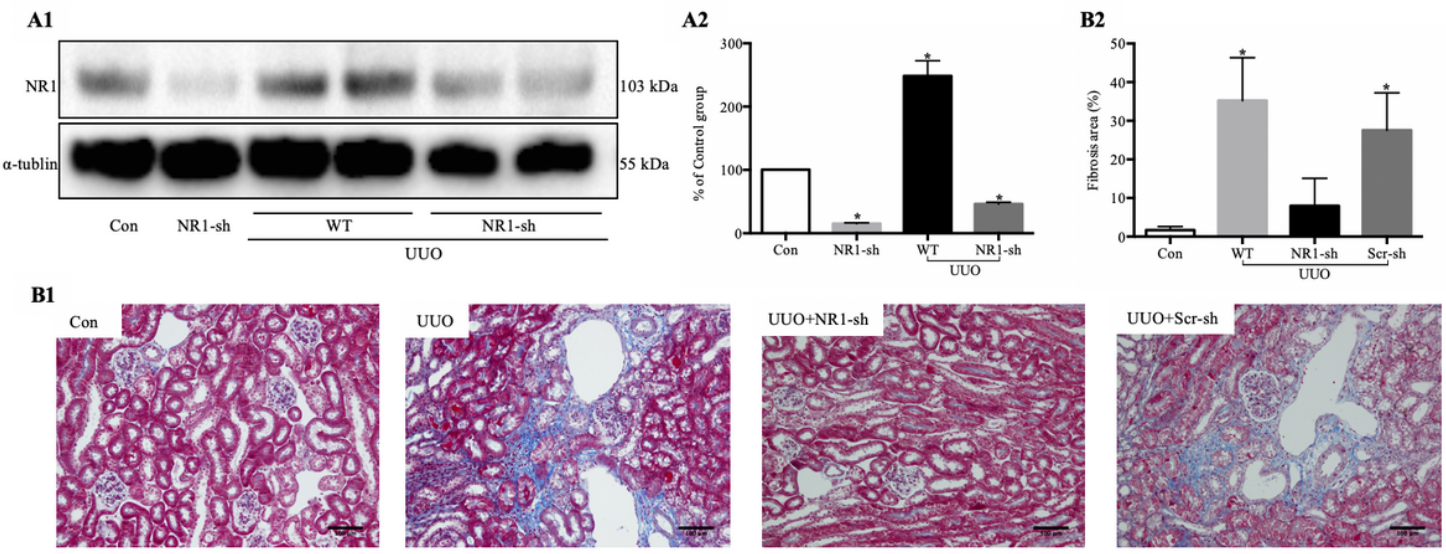

Figure 1

NR1 was overexpressed in UUO-injured kidneys in C57BL/6 mice. (A) Western blots of NR1 expression in Control (Con) group, NR1-targeting shRNA-transfected (NR1-sh) group, UUO group and UUO + NR1-sh group (A1) and band analysis (A2). (B) Masson's trichrome staining of kidneys in Con group, UUO group, UUO + NR1-sh group and UUO + Scr-sh group (B1) and quantification of fibrosis area (%) (B2). n = 6, *P <0.01 versus Con group. Representative images from each group (Origin magnification: ×200. Scale bar = 100 μm).

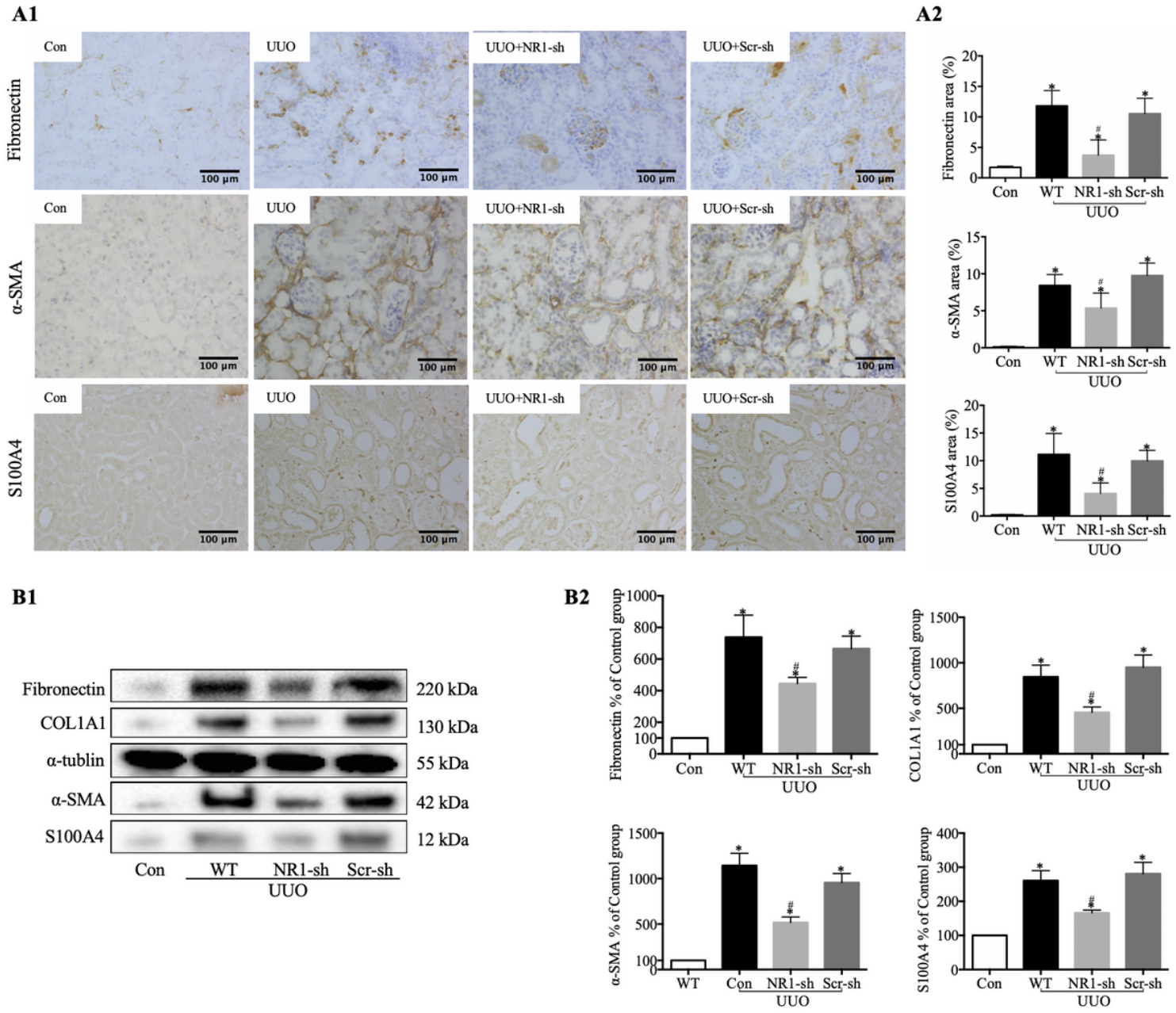

Figure 2

NR1 knockdown partially reverses increased expression levels of fibrotic markers in UUO kidneys. (A) Immunohistochemical staining of fibronectin, α-SMA and S100A4 (A1) and quantitative analysis (A2) of kidneys from Control (Con) group, UUO group, UUO + NR1-targeting shRNA-transfected (NR1-sh) group and UUO + scrambled shRNA transfected (Scr-sh) group. (B) Western blotting of fibronectin, COL1A1, α-SMA and S100A4 COL1A1 (B1) and quantitative analysis (B2). n = 6, *P <0.01 versus Con group, #P <0.01 versus UUO group. Representative images from each group (Origin magnification: ×200. Scale bar = 100 μm).

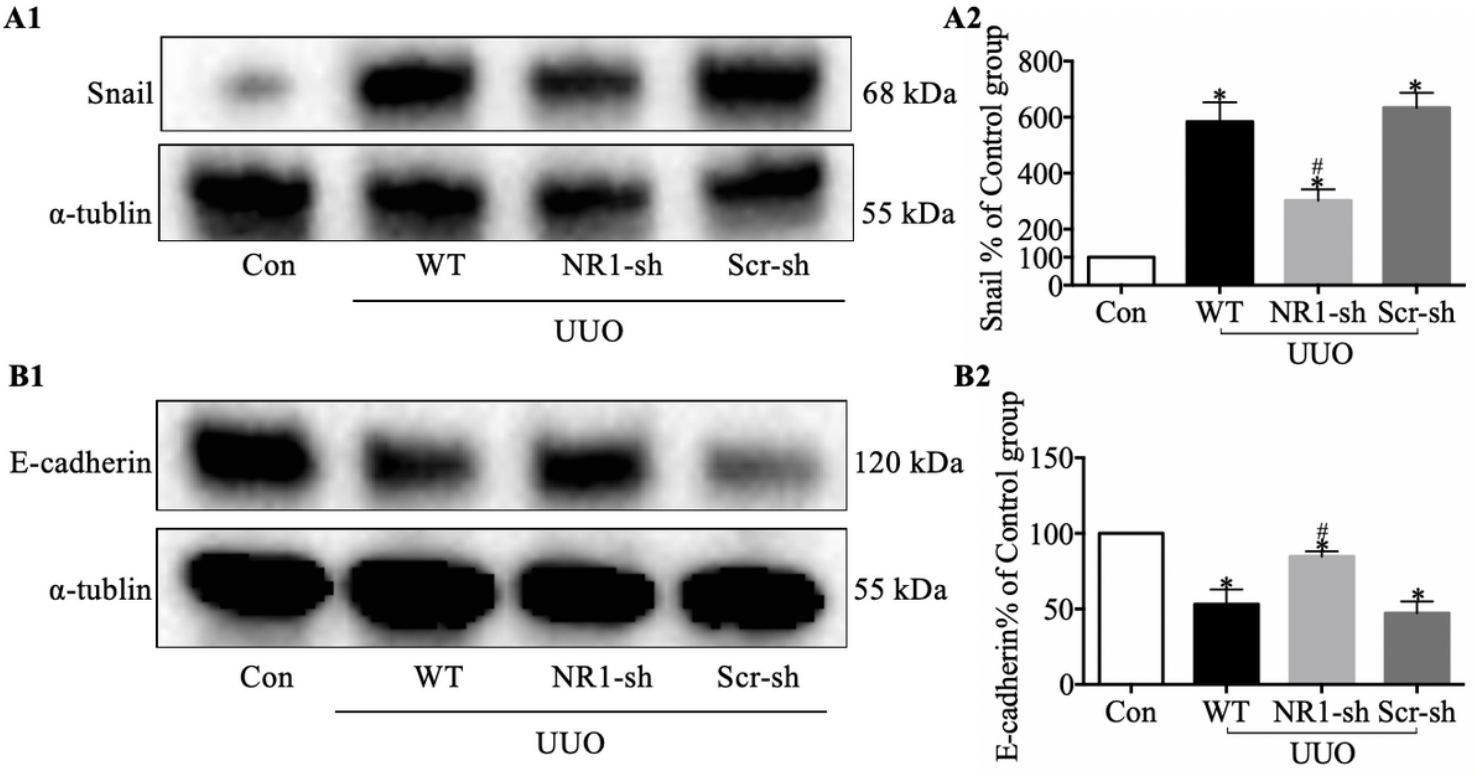

Figure 3

NR1 partially inhibits expression changes in EMT markers after UUO injury. (A) Snail expression changes measured by western blotting for the Control (Con) group, UUO group, NR1-targeting shRNA-transfected (NR1-sh) + UUO group and scrambled shRNA transfected (Scr-sh) + UUO group (A1) and quantitative analysis (A2). (B) E-cadherin (mean ± SEM, n = 6, *P <0.01 versus Con group, #P <0.01 versus UUO group).

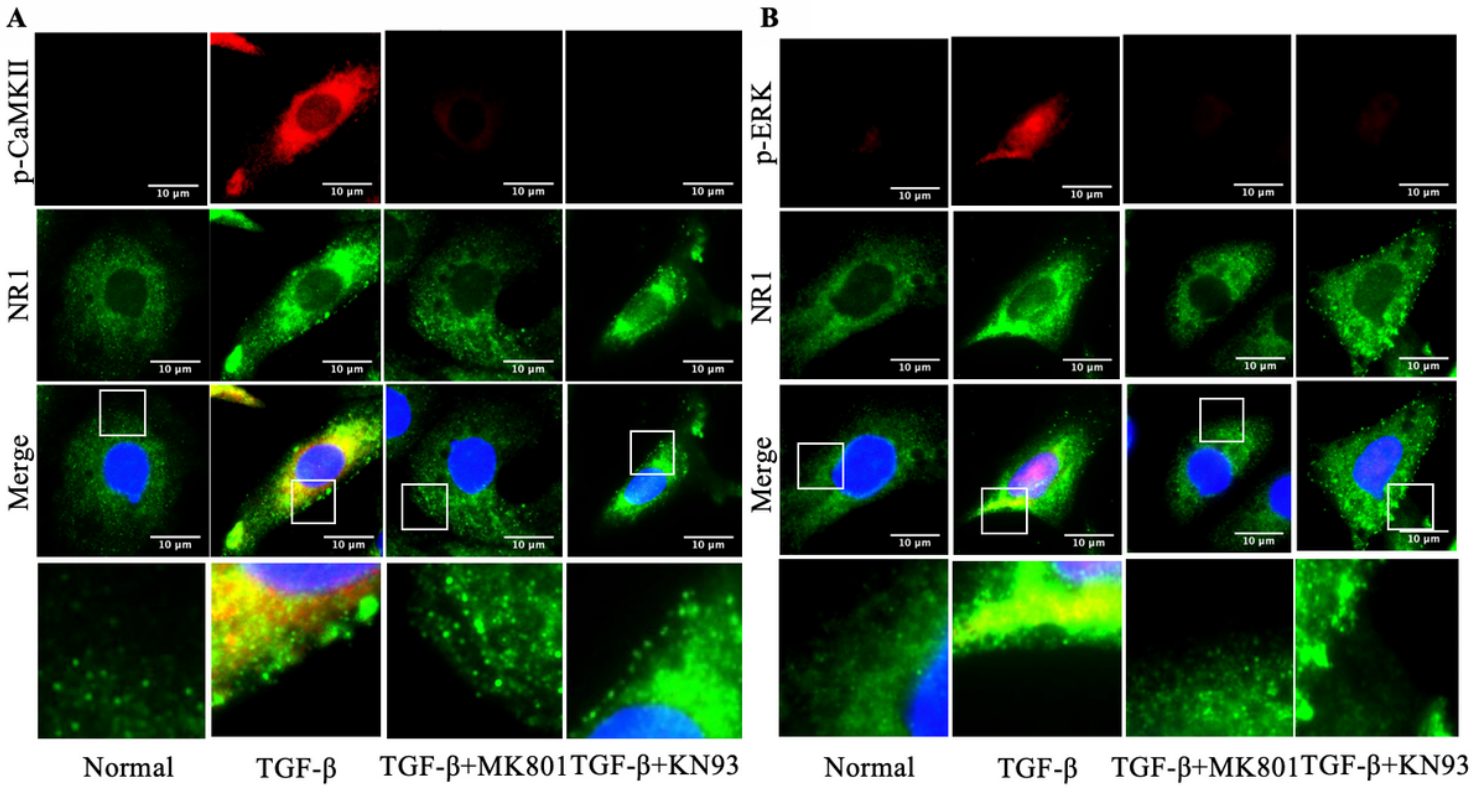

Figure 4

Immunofluorescent images for (A) p-CaMKII (red) and NR1 (green) expression and (B) p-ERK (red) and NR1 (green) expression in HK-2 cells in the normal control group, TGF-β group, TGF-β+MK801 group and TGF-β+KN93 group (Scale bar = 10 μm).

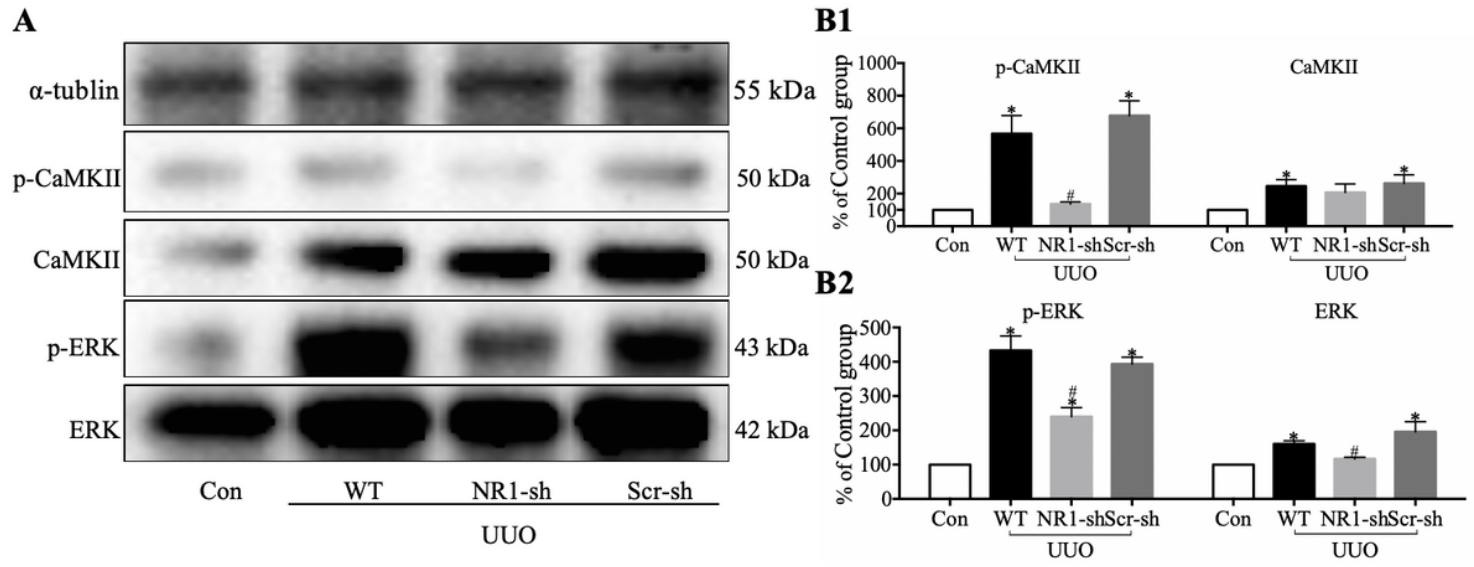

Figure 5

NMDAR activates CaMKII/ERK in UUO-induced renal fibrosis C57BL/6 mice. (A) Western blots for total and p-CaMKII, and total and p-ERK expression levels and (B) band analysis (mean ± SEM, n = 6, *P <0.01 versus Control (Con) group, #P <0.01 versus UUO group).

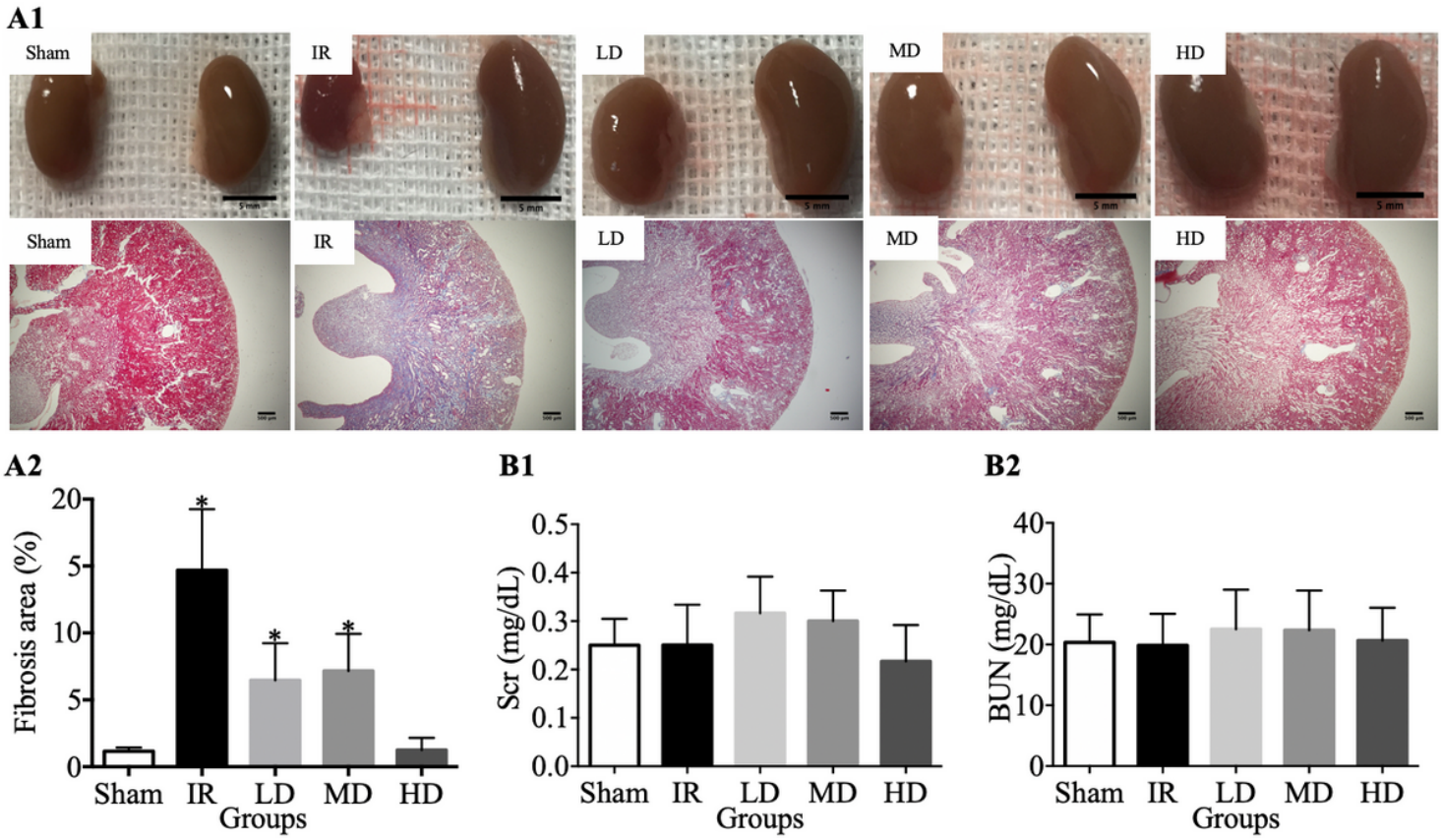

Figure 6

Oral NMDAR inhibitor dextromethorphan protected kidneys from chronic RF after IR injury. (A) Injured kidneys on the left and healthy kidneys on the right with Masson's staining of injured kidneys. (B) Kidney functions. IR group: ischemia/reperfusion group, LD group: low-dose DXM group, MD group: moderate-dose DXM group, HD group: high-dose DXM group. Representative image out of n = 6 individual samples per group. The original magnification of staining images was 40× (Scale bar = 100μm).

Supplementary Files

This is a list of supplementary files associated with this preprint. Click to download.

- ARRIVEGuidelinesChecklist.pdf
- SupplementalFigure1.png